

Atmospheric $p\text{CO}_2$ sensitivity to the biological pump in the ocean

David E. Archer,¹ Gidon Eshel,¹ Arne Winguth,^{1,4} Wallace Broecker,²
Ray Pierrehumbert,¹ Michael Tobis,³ and Robert Jacob¹

Abstract. In models of the global carbon cycle, the $p\text{CO}_2$ of the atmosphere is more sensitive to the chemistry of the high-latitude surface ocean than the tropical ocean. Because sea-surface nutrient concentrations are generally high in the high latitudes, $p\text{CO}_2$ sensitivity to high-latitude forcing also determines $p\text{CO}_2$ sensitivity to the biological pump globally. We diagnose high-latitude sensitivity of a range of ocean models using atmospheric $p\text{CO}_2$ above an abiotic ocean; cold high-latitude waters pull abiotic $p\text{CO}_2$ to low values. Box models are very high-latitude sensitive, while most global circulation models are considerably less so, including a two-dimensional overturning model, two primitive equation models, the Hamburg class of large scale geostrophic (LSG) general circulation models (GCMs), and the MICOM isopycnic GCM. High-latitude forcing becomes more important in a depth-coordinate GCM when lateral diffusion is oriented along isopycnal surfaces, rather than horizontally, following *Redi* [1982]. In two different GCMs (a primitive equation model and LSG), addition of the *Gent and McWilliams* [1990] isopycnal thickness diffusion scheme had only minor impact on high-latitude sensitivity. Using a simplified box model, we show that high-latitude sensitivity depends on a high-latitude monopoly on deep water formation. In an attempt to bridge the gap between box models and GCMs, we constructed a simple slab overturning model with an imposed stream function which can be discretized at arbitrary resolution from box model to GCM scale. High-latitude sensitivity is independent of model resolution but very sensitive to vertical diffusion. Diffusion acts to break the high-latitude monopoly, decreasing high-latitude sensitivity. In the isopycnic GCM MICOM, however, high-latitude sensitivity is relatively insensitive to diapycnal diffusion of tracers such as CO_2 . This would imply that flow pathways in MICOM take the place of vertical diffusion in the slab model. The two nominally most sophisticated ocean models in the comparison are the isopycnic model MICOM and the depth-coordinate GCM with *Redi* [1982] and *Gent and McWilliams* [1990] mixing. Unfortunately, these two models disagree in their abiotic CO_2 behavior; the depth-coordinate isopycnic mixing GCM is high-latitude sensitive, in accord with box models, while MICOM is less so. The rest of the GCMs, which have historically seen the most use in geochemical studies, are even less high-latitude sensitive than MICOM. This discrepancy needs to be resolved. In the meantime, the implication of the MICOM/traditional GCM result would be that box models overestimate high-latitude sensitivity of the real ocean. This would eliminate iron dust fertilization of the ocean as an explanation for the glacial $p\text{CO}_2$ range of 180-200 μatm [Archer *et al.*, 2000].

1. Introduction

The equilibrium partial pressure of CO_2 exerted by surface seawater (its $p\text{CO}_2$), is greater than atmospheric $p\text{CO}_2$ in some parts of the ocean and undersaturated in other parts. One factor

generating heterogeneity of sea surface $p\text{CO}_2$ is temperature; the solubility of CO_2 decreases with increasing temperature, so the $p\text{CO}_2$ of a cold sea water sample goes up when it warms. Biological activity also affects seawater $p\text{CO}_2$ by redistributing carbon and the nutrients NO_3 and PO_4^{3-} in the water column, resulting in a correlation (at constant temperature) between $p\text{CO}_2$ and nutrient concentration. Surface water $p\text{CO}_2$ can be altered by CO_2 exchange with the atmosphere, if the residence time of surface waters is longer than the gas exchange equilibration time. The steady state $p\text{CO}_2$ of the atmosphere is an average of the steady state sea surface $p\text{CO}_2$ field weighted by area and by the kinetics of gas exchange.

The simplest models of the ocean carbon cycle that resolve the large-scale chemical and thermal heterogeneity of the real ocean are the box models. The ocean is divided into a handful of reservoirs (numbering three to tens) which are internally well mixed. Seawater is exchanged between boxes by

¹Department of the Geophysical Sciences, University of Chicago, Illinois.

²Lamont-Doherty Earth Observatory of Columbia University, Palisades, New York.

³Space Science and Engineering Center, University of Wisconsin, Madison, Wisconsin.

⁴Now at Department of Atmospheric and Oceanic Sciences, University of Wisconsin, Madison.

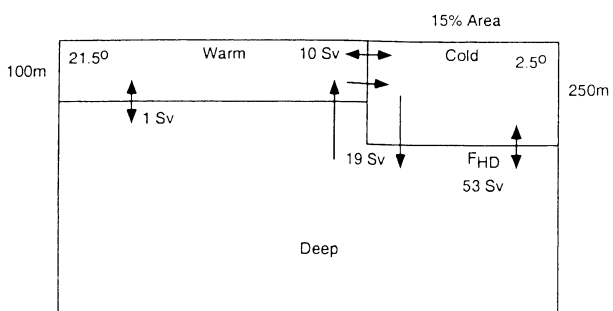


Figure 1. The three-box model of the ocean carbon cycle. The sea surface is divided into high latitudes (15% of the ocean area) and low latitudes, which extend to 250 and 100 m depth, respectively. Thermohaline circulation is imposed as a cyclic flow of 19 Sv, supplemented by exchange fluxes between boxes, the most significant of which connects the high-latitude and deep ocean reservoirs (F_{HD}), of 53 Sv.

imposing rates of fluid flow and exchange between them. The simplest of these is the high-latitude outcrop model (Figure 1), presented by three groups [Knox and McElroy, 1984; Sarmiento and Toggweiler, 1984; Siegenthaler and Wenk, 1984; Toggweiler and Sarmiento, 1985]. More boxes can be added in order to resolve distinctions in water chemistry and circulation between northern and southern component deep water, and between intermediate and thermocline water reservoirs.

In steady state, the $p\text{CO}_2$ of the atmosphere over the three-box ocean is extraordinarily sensitive to changes in the temperature and nutrient chemistry of the high-latitude surface box and relatively insensitive to forcing from low latitudes [Knox and McElroy, 1984; Sarmiento and Toggweiler, 1984; Siegenthaler and Wenk, 1984; Toggweiler and Sarmiento, 1985]. This is significant because high-latitude surface waters are cold and contain high concentrations of nutrients, so that increasing the effectiveness of biological uptake (the steady sea surface nutrient concentration) could decrease sea surface $p\text{CO}_2$ to very low levels. Iron fertilization of high latitudes has been proposed as an explanation for low glacial $p\text{CO}_2$ values [Martin and Fitzwater, 1988] and as a potential means of extracting fossil fuel CO_2 from the atmosphere in the future [Peng and Broecker, 1991; Sarmiento and Orr, 1991]. The insensitivity of the steady state atmosphere to low-latitude temperature and nutrient chemistry would also imply that changes in tropical sea surface temperature, either in the past or in the future, would have little direct effect on atmospheric $p\text{CO}_2$.

A second category of ocean carbon cycle models is the general circulation models (GCMs), which discretize the ocean into a finite difference grid, usually with resolution of 3° of latitude/longitude or smaller. The circulation is a numerical approximation to the Navier Stokes equations for fluid flow on a stratified rotating sphere. Two types of GCMs will be considered. Depth-coordinate GCMs discretize the properties of the water column onto surfaces of constant depth, typically into 10-15 levels, more closely spaced near the sea surface to better resolve the upper ocean and the thermocline. Isopycnic GCMs discretize the fluid properties along isopycnal (constant

density) surfaces, the depth of which evolve in time with changes in the density field of the ocean. The advantage of isopycnic ocean models is the elimination of most of the cross-grid vertical flow, enabling explicit control of diapycnal diffusion. Because of computational limits, none of the GCMs shown here resolve the eddies, fronts, or internal waves that are responsible for mixing in the real ocean.

2. A Discrepancy in High-Latitude Sensitivity

This study began with the unexpected observation that the atmospheric $p\text{CO}_2$ over the Hamburg Ocean Carbon Cycle Model version 2 (HAMOCC2), a depth-coordinate GCM carbon cycle model, is much less sensitive to biological uptake of

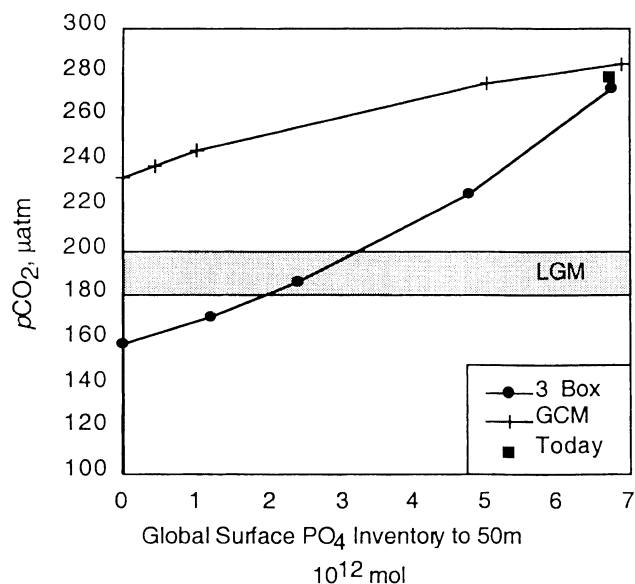


Figure 2. Full biological model $p\text{CO}_2$ as a function of sea surface nutrients. The HAMOCC2 GCM advects tracers off-line using the annual mean flow field from the large scale geostrophic (LSG) physical flow model, using an implicit upstream advection method over a time step of one year [Maier-Reimer and Bacastow, 1990] (plusses). The global inventory of PO_4 in the top 50 m of the ocean (the top box at each grid point) correlates with the steady state $p\text{CO}_2$ of the atmosphere. Circles indicate the three-box model results (Figure 1). The present-day configuration specifies $1.4 \mu\text{M}$ PO_4 in the high-latitude box and $0.2 \mu\text{M}$ in the low latitudes. These were varied by scaling both simultaneously down to zero (complete nutrient limitation). Squares indicate preanthropogenic $p\text{CO}_2$ from the Vostok ice core [Barnola et al., 1987], plotted against the present-day sea surface inventory of PO_4 , from [Levitus et al., 1993]. Sea ice is diagnosed as annual mean temperatures $< 0^\circ\text{C}$, a cutoff which generates comparable ice cover to the HAMMOC model. The crossover point between the two models is close to present-day conditions not because this is the only point where modelers know the answer in advance but because the high nutrient concentration of high-latitude surface waters counteracts the colder temperatures there, reducing the $p\text{CO}_2$ contrast between high- and low-latitude surface waters. The models get the right answer regardless of whether the atmospheric $p\text{CO}_2$ is determined by high- or low-latitude surface forcing.

carbon than is a box model of the ocean chemistry (Figure 2). Both models were tuned to predict the preanthropogenic $p\text{CO}_2$ [Barnola et al., 1987] when the sea surface inventory of PO_4 is close to the Levitus et al. [1993] value, and both predict a decrease of $p\text{CO}_2$ with decreasing sea surface nutrient concentration (increasing biological pump). However, the minimum $p\text{CO}_2$ predicted by the GCM is 233 μatm , while the box model reaches 158 μatm , when sea surface PO_4 is depleted (the limit of the biological pump). The nutrient inventory/ $p\text{CO}_2$ comparison between the two models may be influenced somewhat by the distribution of sea surface nutrients, which are explicitly concentrated in the high-latitude box in the three-box model but less controlled in the GCM. However, the completely nutrient-depleted states of the two models ought to be comparable in this regard. Instead, we see a vast difference in the predicted sensitivity of atmospheric $p\text{CO}_2$ to biological forcing from the ocean.

At first we wondered whether the different sensitivities to the biological pump were caused by differences in the biological components of the models. To test for this, we eliminated biological effects altogether, and lowered the mean CO_2 concentration of the ocean to compensate. The effect of the biological pump in the ocean is to strip upwelling surface waters of nutrients and their associated "metabolic" carbon and alkalinity. Instead of removing these constituents every time the water upwells, the abiotic experiment removes the biological constituents from the whole ocean in the initial condition.

Abiotic $p\text{CO}_2$ is identical to nutrient-limited $p\text{CO}_2$ if the following conditions are met. In the biological model, no biological sources or sinks of alkalinity, and strictly Redfield stoichiometry in the production and dissolution of organic carbon. In the abiotic model, removal of nutrients and a Redfield equivalent of mean total CO_2 . In HAMOCC2 the addition of nutrients and metabolic carbon in this ratio changes $p\text{CO}_2$ by less than 0.1 μatm from the abiotic value, when organic carbon production is nutrient-limited and CaCO_3 production is forbidden. When the alkalinity pump and non-Redfield stoichiometry are added, the correct metabolic recipe depends on details of the biological cycling in the model. The classical recipe might decrease total CO_2 by 233 $\mu\text{mol kg}$ and alkalinity 116 $\mu\text{eq kg}$, associated with 2.2 of PO_4^{3-} draw down and CaCO_3 :organic C production ratio of 0.25. The exact values for any model depend on the response of CaCO_3 production to organic carbon fertilization, fractionation between organic carbon and CaCO_3 as they dissolve in the water column, and any non-Redfield production or redissolution stoichiometry for organic carbon.

Because details of the biological pumps vary between ocean models, no single metabolic recipe will be quantitatively correct for all models. We arbitrarily chose a metabolic recipe intended to generate roughly comparable chemistry at the sea surface to the nutrient-limited state, and will interpret the results qualitatively as predictors of the nutrient-limited $p\text{CO}_2$. We use an initial condition of 2371 $\mu\text{eq kg}$ alkalinity, of 2085 $\mu\text{mol kg}$ total CO_2 , no nutrients or biological pump, and atmospheric $p\text{CO}_2$ of 278 μatm . In practice, for HAMOCC2, the Princeton model, and the 3-Box model, abiotic $p\text{CO}_2$ – 69 μatm predicts nutrient-limited $p\text{CO}_2$ to within 12 μatm [T. Hughes, personal communication, 1998]. The advantage of

the abiotic $p\text{CO}_2$ diagnostic is that it eliminates differences in biological cycling (both the organic carbon and the CaCO_3 pumps) between different models. We can run the diagnostic on circulation models for which biological models have not yet been developed (for example, the MICOM isopycnic ocean model).

The three-box model reached abiotic $p\text{CO}_2$ equilibrium at 219 μatm , while the HAMOCC GCM equilibrated at 293 μatm (Figure 3). Abiotic $p\text{CO}_2$ is a diagnostic for high-latitude $p\text{CO}_2$ sensitivity because $p\text{CO}_2$ is a strong function of temperature. If the high-latitude ocean controls $p\text{CO}_2$, then abiotic $p\text{CO}_2$ of the atmosphere is low, reflecting equilibrium with cold seawater. The box model atmosphere would be in equilibrium with the average chemistry of the ocean at a temperature of $\sim 7.5^\circ\text{C}$, indicative of high-latitude control. The equilibrium temperature of HAMOCC is $\sim 14^\circ\text{C}$, reflecting a greater low-latitude influence. These results are consistent with comparisons of box model versus GCM $p\text{CO}_2$ sensitivity to low-latitude temperature [Bacastow, 1996] and low-latitude CO_2 solubility [Broecker et al., 1999].

The 74 μatm difference in abiotic $p\text{CO}_2$ is analogous to the difference between the two nutrient-limited $p\text{CO}_2$ models in Figure 2 (75 μatm). The contrasting sensitivity to the biological pump (Figure 2) was not caused by biology after all but rather by transport of CO_2 within the model oceans. High-latitude control of $p\text{CO}_2$ acts to amplify the effect of the biological pump on $p\text{CO}_2$ because high-latitude surface waters have more nutrients to lose and because CO_2 is more soluble in cold seawater. High-latitude sensitivity leverages the impact of the global biological pump on atmospheric $p\text{CO}_2$.

Both types of ocean models do an adequate job of simulating the present-day ocean, (albeit in practice with a bit of tuning) but diverge strongly as nutrients are depleted. This is because metabolic carbon compensates for the high solubility of CO_2 in cold high-latitude surface water. If nutrient-limited seawater (say, the composition of the mean ocean initial condition for the abiotic experiments described above) is cooled from 25° to 0°C , $p\text{CO}_2$ would drop from 424 to 145 μatm . If we then add 1.4 μM PO_4^{3-} and associated Redfield metabolic carbon (with no change in alkalinity), $p\text{CO}_2$ increases to 332 μatm . In an ocean with biological cycling, it makes less difference which part of the surface ocean controls atmospheric $p\text{CO}_2$. The model gets close to the right answer regardless. As nutrients are depleted or eliminated, $p\text{CO}_2$ of the high latitudes decreases, and the models diverge.

We computed abiotic $p\text{CO}_2$ over a variety of ocean models and found a wide range of values. Box models include Pandora with 10 boxes [Broecker and Peng, 1987], the Cyclops with 13 [Keir, 1988], and the Michel model, derived from the flow field of the LSG GCM, with 19 [Michel et al., 1995]. "Continuum" circulation models include a two-dimensional zonal mean model [Stocker et al., 1992], two primitive equation GCMs (Princeton [Murnane et al., 1999], and OM3), the large scale geostrophic family (LSG and HAMOCC2 [Maier-Reimer and Bacastow, 1990; Winguth et al., 1994]), and an isopycnic GCM (MICOM [Bleck et al., 1995]). Variations include the orientation of lateral diffusion along isopycnal surfaces (OM3/Isopyc [Redi, 1982]) and the Gent and McWilliams [1990] "isopycnal thickness diffusion" eddy

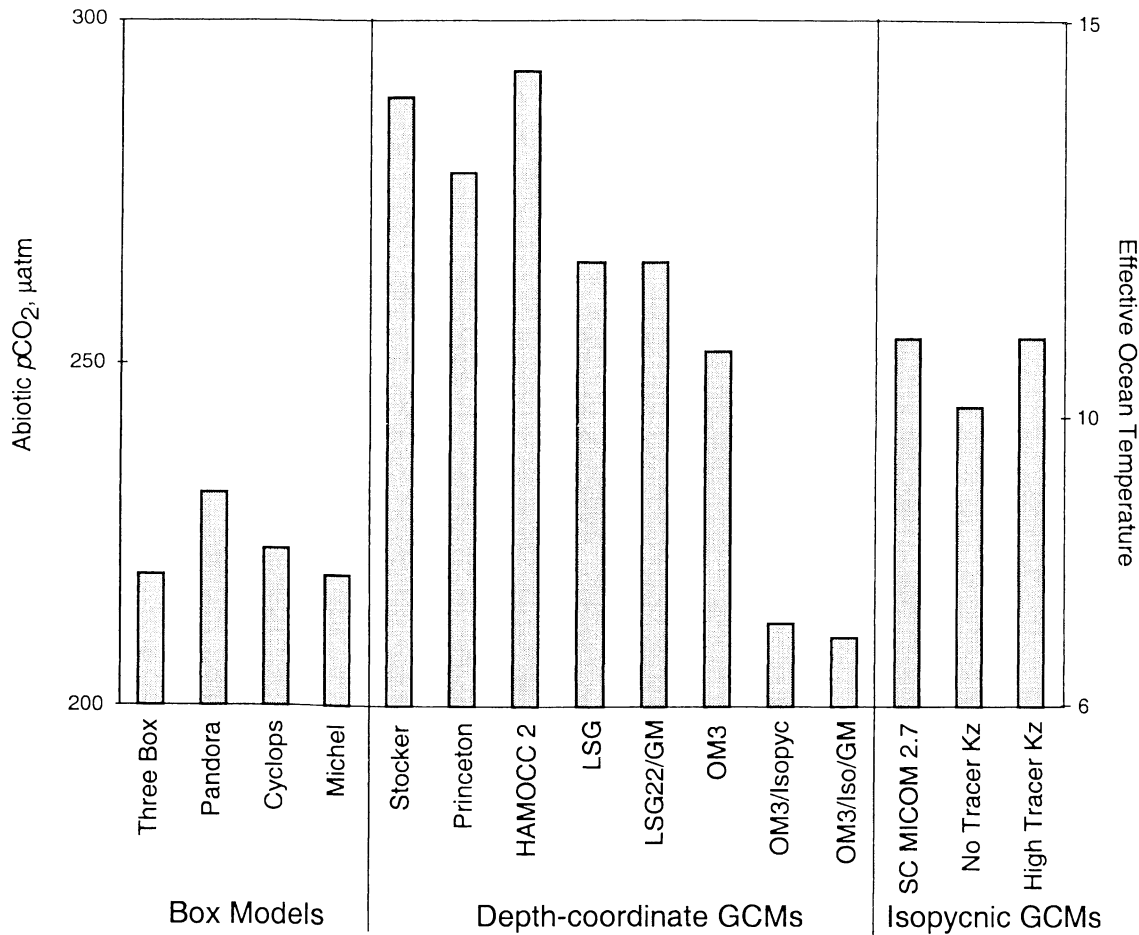


Figure 3. Abiotic $p\text{CO}_2$ model results are intended to be a simpler analog for the case of sea surface nutrient depletion, enabling comparison of a range of box models and GCMs. See Appendix for computation details.

mixing parameterization (OM3/Iso-GM and LSG22/GM). Details of the model configurations are given in the Appendix.

All of the box models (Pandora, Cyclops, and Michel) generate abiotic $p\text{CO}_2$ between 220–230 μatm , consistent with the three-box model. All of the GCMs, with one exception, give abiotic $p\text{CO}_2$ between 250 and 295 μatm . The exception is the primitive equation model OM3 when lateral diffusion is oriented along isopycnal surfaces, following Redi [1982]. After reorientation of the diffusion tensor, addition of the Gent/McWilliams isopycnal thickness diffusion scheme had little further effect on abiotic $p\text{CO}_2$.

3. Cause of the Discrepancy

Where does the variability in high-latitude sensitivity come from? The strongest distinction seems to be between box models and continuum models of ocean circulation. Interestingly, the Michel 19-box model was based directly on the flow field of the LSG GCM [Maier-Reimer and Bacastow, 1990], but the high-latitude sensitivity of the box version of the model is completely different from that of the GCM. We labored extensively to construct a box model that would capture GCM high-latitude sensitivity. First we followed the

Michel *et al.* [1995] strategy, binning grid points from the LSG GCM and summing fluxes. An ambiguity here was whether to use net or gross fluxes between adjacent boxes. We tried running color and age tracer experiments in HAMOCC2, which we then used to tune a box model using inverse techniques. Construction of a box model which is able to mimic the geochemistry and high-latitude sensitivity of the GCM proved to be remarkably difficult. The best we can offer is to explain the mechanism behind high-latitude sensitivity using a simplified three-box model. Then we construct a model designed to span the range between box models and continuum models, to explore the distinction between the two model types.

3.1. Simplest High-Latitude Sensitive Ocean Model

The configuration of the original three-box model (Figure 1) suggests to the casual inspector that the high-latitude surface ocean controls $p\text{CO}_2$ because it is rapidly replenished by mixing with the deep sea (F_{hd} in Figure 1). However, we find that F_{hd} can be eliminated without losing high-latitude sensitivity. Abiotic $p\text{CO}_2$ over a three-box model with overturning circulation only is still high-latitude driven, with

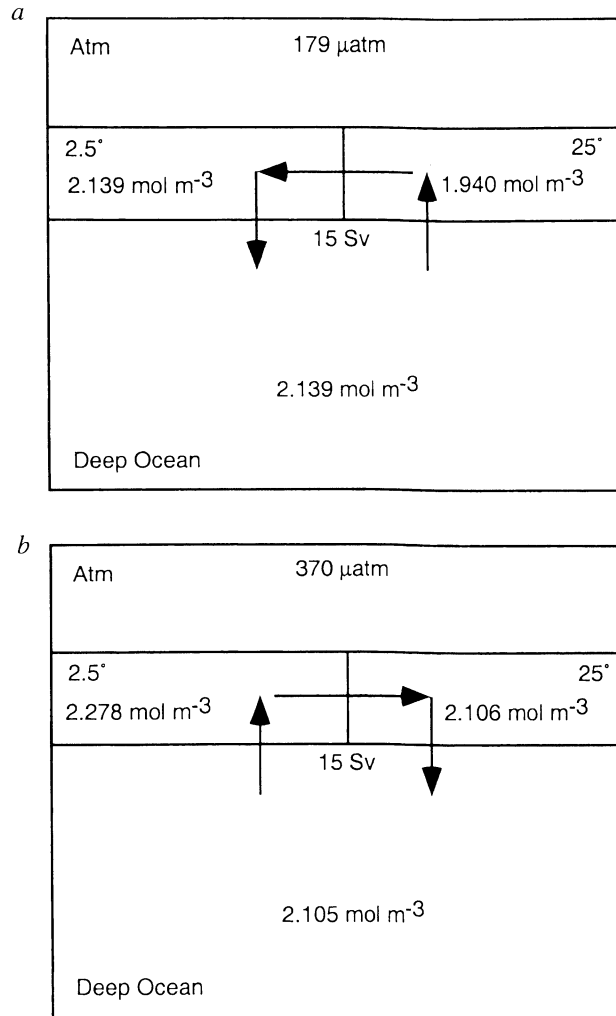


Figure 4. A demonstration of the mechanism behind the high-latitude sensitivity of nondiffusive ocean models. (a) Eliminating the geometrical asymmetry between the high- and low-latitude surface boxes and all but the overturning circulation, the model retains its high-latitude sensitivity, as demonstrated by the low abiotic $p\text{CO}_2$. (b) When the direction of the overturning circulation is reversed, the low latitudes control $p\text{CO}_2$.

abiotic $p\text{CO}_2$ of only $179 \mu\text{atm}$ (Figure 4a). However, when the direction of overturning is reversed (Figure 4b), the steady state $p\text{CO}_2$ increases dramatically to $370 \mu\text{atm}$. When the circulation is run backward, the low latitudes control $p\text{CO}_2$.

This behavior can be understood as follows: the concentration of CO_2 in the deep sea, the largest carbon reservoir in the system, remains close to the mean ocean concentration in both cases. In the steady state, the downwelling surface box must have a CO_2 concentration equal to the deep-sea concentration because with the elimination of the biological pump there are no other sources of carbon to the deep sea. The downwelling surface concentration is therefore closely pinned to the ocean mean, while the upwelling surface box is not constrained in this way and yields to atmospheric

$p\text{CO}_2$ forcing. The atmosphere equilibrates with the mean ocean chemistry at the temperature of the downwelling box. The high-latitude sensitivity mechanism therefore relies on a high-latitude monopoly of deep water formation.

The chemical constraint is that the chemistry of the high-latitude surface remains close to the ocean mean, if the high latitude controls the formation of deep water in the ocean. In contrast to this box model result, the high-latitude CO_2 concentration in the HAMOCC GCM is higher than the ocean mean (Figure 5). The effective equilibrium temperature is by definition the equilibrium temperature with the mean chemistry of the ocean, plotted for all of the model results in Figure 3. Nearly all of the GCMs cluster in the range $11\text{--}14^\circ$, in comparison with box models between 7° and 8° .

How do GCMs defeat the high-latitude sensitivity of the box models? To explore this question, we constructed a simple slab circulation model that is able to span the resolution range between GCMs and box models (Plate 1). The ocean is treated as a single zonal slab 180° wide and ranging from 70°S to 30°N . Flow velocities are derived from an analytically defined stream function chosen to mimic the typical magnitude and flow pattern of the overturning circulation generated by GCMs. Specifying the flow, rather than predicting it based on physics as in a GCM, minimizes the sensitivity of the flow field to changes in grid resolution. Sea surface temperature (SST) is fixed to a smoothly varying function of latitude ranging from 25°C at the equator to 2°C at 70°S . The stream function and SST function are discretized at resolutions ranging from 50×100 grid points (reducing numerical diffusion to negligible levels), down to 2×2 , essentially a box model. The vertical grid is stretched at low resolution to resolve a 100 m thick surface layer, and the horizontal grid resolves the high latitudes ($70^\circ\text{--}50^\circ\text{S}$), even at 2×2 box

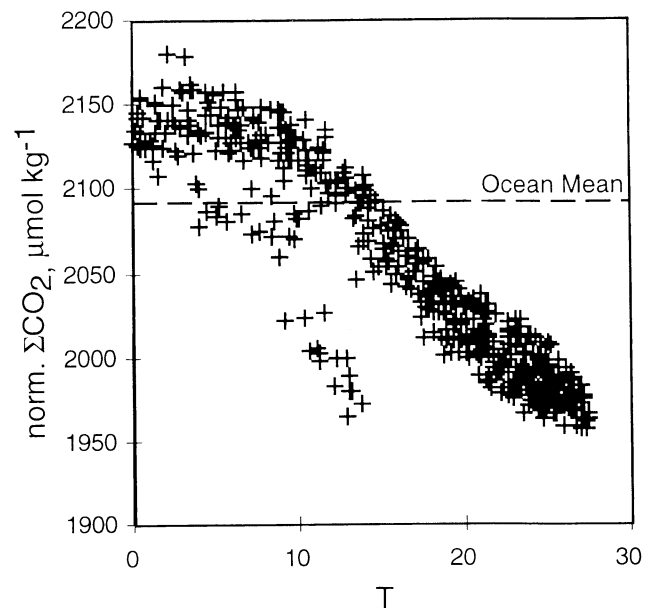


Figure 5. Sea surface total CO_2 concentrations from HAMOCC, normalized to constant salinity, plotted against sea surface temperature (SST). The effective temperature of this GCM is 15° (see Figure 3).

resolution. Tracer advection is modeled using the upstream method, which is more diffusive than center differencing, but is ubiquitous in box models. Convection mixes water properties vertically when colder water overlies warmer water. Mixing is parameterized as diffusion, with distinct horizontal and vertical rates. The three tracers are temperature, age (a simplified analog to C in the real ocean), and total CO_2 concentration (the sum of all the oxidized carbon species concentrations). The alkalinity and salinity of the water are assumed constant. Atmospheric $p\text{CO}_2$ is determined by the area-weighted fluxes from the surface ocean.

Temperature, age, and total CO_2 sections from the slab model at high resolution are shown in Plate 1. When diffusion is imposed ($K_h = 10\text{ m s}$ and $K_v = 10\text{ m s}$), the model captures the essential features of the ocean: the structure of the thermocline and the age and temperature of the abyss. The model also generates an abiotic $p\text{CO}_2$ typical of depth-coordinate GCMs. Abiotic $p\text{CO}_2$ is only slightly sensitive to model resolution (Plate 2a) but extremely sensitive to diffusion (Plate 2b).

The 2×2 box model is also shown in Plate 1. The effects of diffusion in this model are represented as exchange fluxes of water, in Sverdrups, between adjacent boxes, added to 12 Sv of overturning circulation. The two high-latitude boxes in this model are mixed by convection, effectively merging into a single box. Vertical diffusion mixes the chemistry of the two boxes as effectively as would an upwinded advective exchange flux of 8 Sv between the low-latitude sea surface and the deep sea. The cold temperature of the deep sea is maintained by deep horizontal diffusion from the convective tower in high latitudes.

The diffusive box model escapes the high-latitude sensitivity exhibited by the overturning three-box model (Figure 4) by breaking the high-latitude monopoly on deep water formation. The deep low latitude box is still close to the ocean average CO_2 concentration, but the high-latitude surface CO_2 concentration exceeds the mean ocean concentration, in contrast to the overturning box model results in Figure 4. The deep-sea chemistry is composed of an average between low-latitude and high-latitude surface waters, weighted by the respective rates of deep water formation.

3.2. Rules of Thumb for Relating the Sea Surface to the Atmosphere

The atmospheric $p\text{CO}_2$ impact of a change in sea surface CO_2 forcing in some region of the ocean, say a change in nutrient concentration or temperature, depends on where the change takes place. Some regions of the surface ocean are more influential of the atmosphere than other regions. We demonstrate the effect using the slab model by measuring the atmospheric $p\text{CO}_2$ response to perturbations in the sea surface forcing as a function of latitude. The ocean surface was divided into 10 equally sized subregions. From each region in turn we imposed an additional flux of CO_2 to the atmosphere, as if the $p\text{CO}_2$ of the surface water in that region were $100\ \mu\text{atm}$ higher than the actual model value. When this is done over all subregions simultaneously, in the new steady state atmospheric $p\text{CO}_2$ increases by $\sim 100\ \mu\text{atm}$. The average response to a perturbation covering 10% of the ocean surface is close to $100\ \mu\text{atm} \times 10\% = 10\ \mu\text{atm}$. The atmospheric response factor of a subregion is defined to be the steady state response divided by the expected $10\ \mu\text{atm}$ average response.

The response factor of the tropics is conceptually and numerically similar to the Harvardton Bear Equilibration Index of Broecker *et al.* [1999].

When diffusion is neglected, the southernmost 10% of the ocean is 8 times more effective than the average for the surface ocean as a whole. This factor decreases to 2.5 when diffusion is increased to $K_v = 1\text{ cm s}$ (Figure 6a). The response factors are plotted cumulatively and normalized to 100% (Figure 6b) to show that when diffusion is neglected, the surface ocean poleward of 60°S enjoys 95% control of atmospheric $p\text{CO}_2$. When a low rate of diffusion is imposed (0.1 cm s), the impact factor of Southern Ocean waters drops somewhat, but the Southern Ocean still dominates $p\text{CO}_2$. However, when diffusion is increased to 1 cm s , the impact of this region drops to 30%, still important but no longer dominant. It should be possible to estimate the effect of some hypothetical change in sea surface nutrients or temperature on equilibrium paleoatmospheric $p\text{CO}_2$ using these sorts of "impact factors," circumventing the need to run circulation models.

4. What is the High-Latitude Sensitivity of the Real Ocean?

We are faced with a discrepancy between the high-latitude $p\text{CO}_2$ sensitivity of box models and continuum models of ocean chemistry. Chemical oceanographic modeling is grounded in box models because of their simplicity and transparency, and box models are widely today used in chemical oceanography and paleoceanography. General circulation models are constrained by geophysical fluid dynamics and are analogous to the atmospheric models that are used to predict the weather every day. Ocean GCMs suffer from inadequate resolution to resolve eddies and from artificial

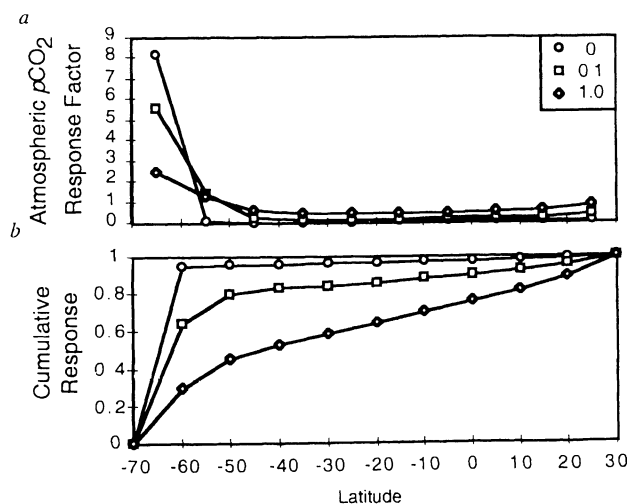


Figure 6. A measure of the abiotic $p\text{CO}_2$ sensitivity to sea surface forcing as a function of latitude. K_v and K_h values are 0 (labeled "0"), 10 and 10 m s (labeled "0.1"), and 10 and 10 (labeled "1"). (a) Sensitivity of atmospheric $p\text{CO}_2$ relative to the expected response to a perturbation of an average subarea of the ocean surface. (b) Cumulative response factors, normalized to a sum of 1.00, showing the sensitivity to high- and low-latitude forcing.

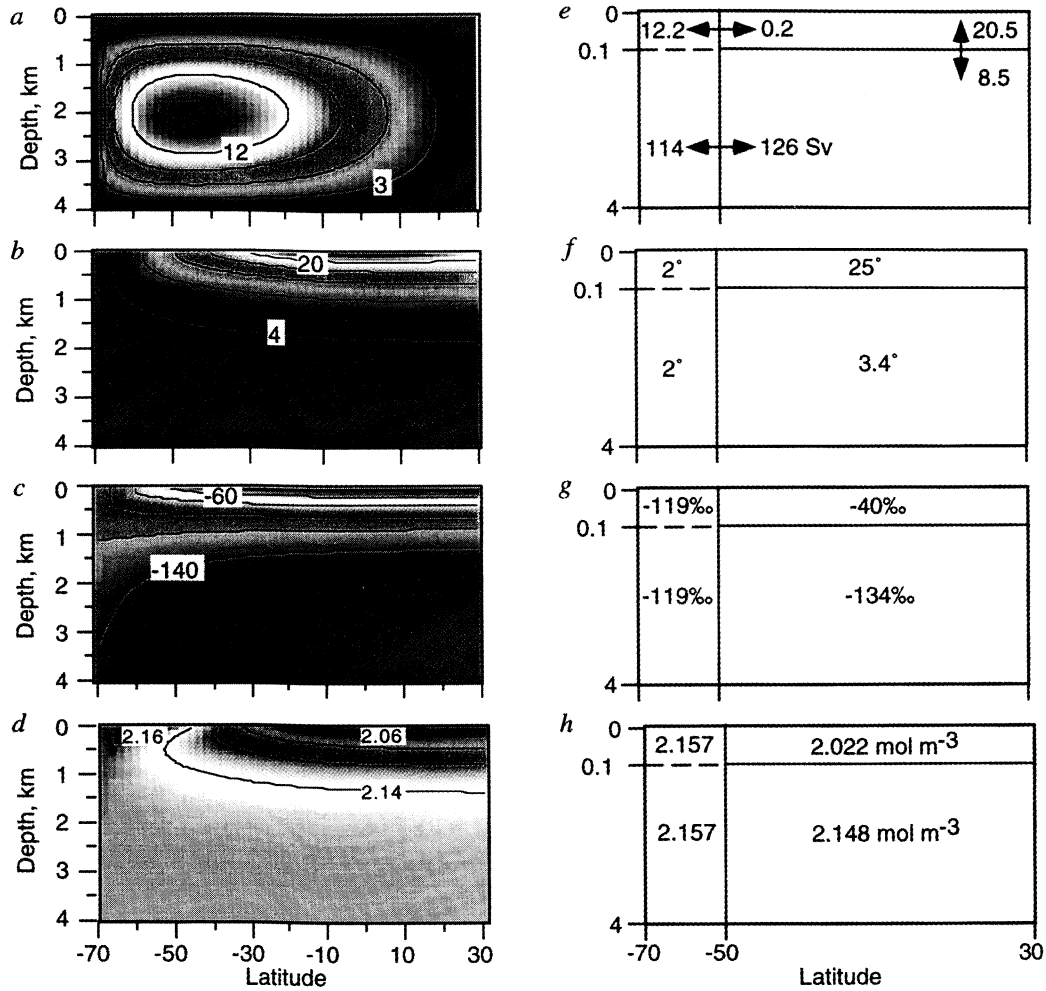


Plate 1. Slab model results. The high-resolution grid (50 by 100 grid points) was chosen to minimize numerical diffusion (K_h is of order 10 m s , and K_z is $2 \times 10 \text{ m s}$ in the upwelling zone). (a) The imposed overturning stream function from which a nondivergent velocity field was derived. (b) Temperature, (c) C age, and (d) total CO_2 concentration. At low resolution (2×2) the model grid is stretched so that the surface ocean and the high latitude are resolved (the minimum cell thickness at the sea surface is 100 m : not to scale), and the minimum cell width is 20° latitude at the southern end of the domain). The temperatures of the surface boxes are the extreme values of the high resolution SST field: 2° and 25°C . The flow field including diffusive fluxes parameterized as exchange fluxes in Sv (e), (f) temperature, (g) C age, and (h) total CO_2 concentration.

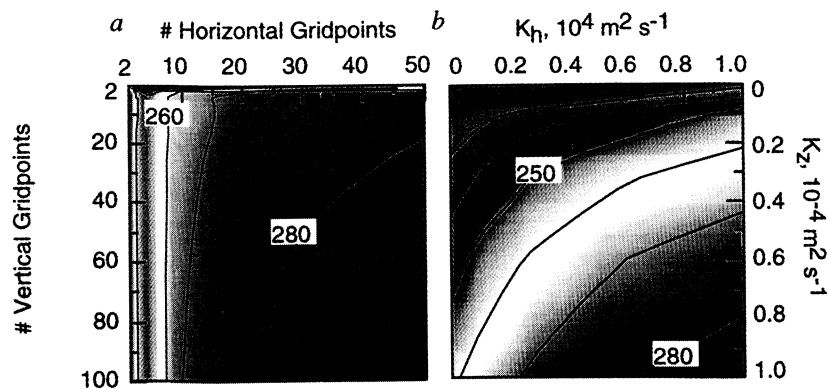


Plate 2. Sensitivity of ocean forcing of atmospheric $p\text{CO}_2$ to grid resolution and vertical and horizontal diffusion. (a) Abiotic $p\text{CO}_2$ is relatively insensitive to model resolution (number of grid points) in latitude and depth. $K_z = 10 \text{ m s}$, $K_h = 10 \text{ m s}$. (b) Abiotic $p\text{CO}_2$ is however very sensitive to imposed diffusion upon the 50×100 grid model. Numerical diffusion is negligible at this resolution.

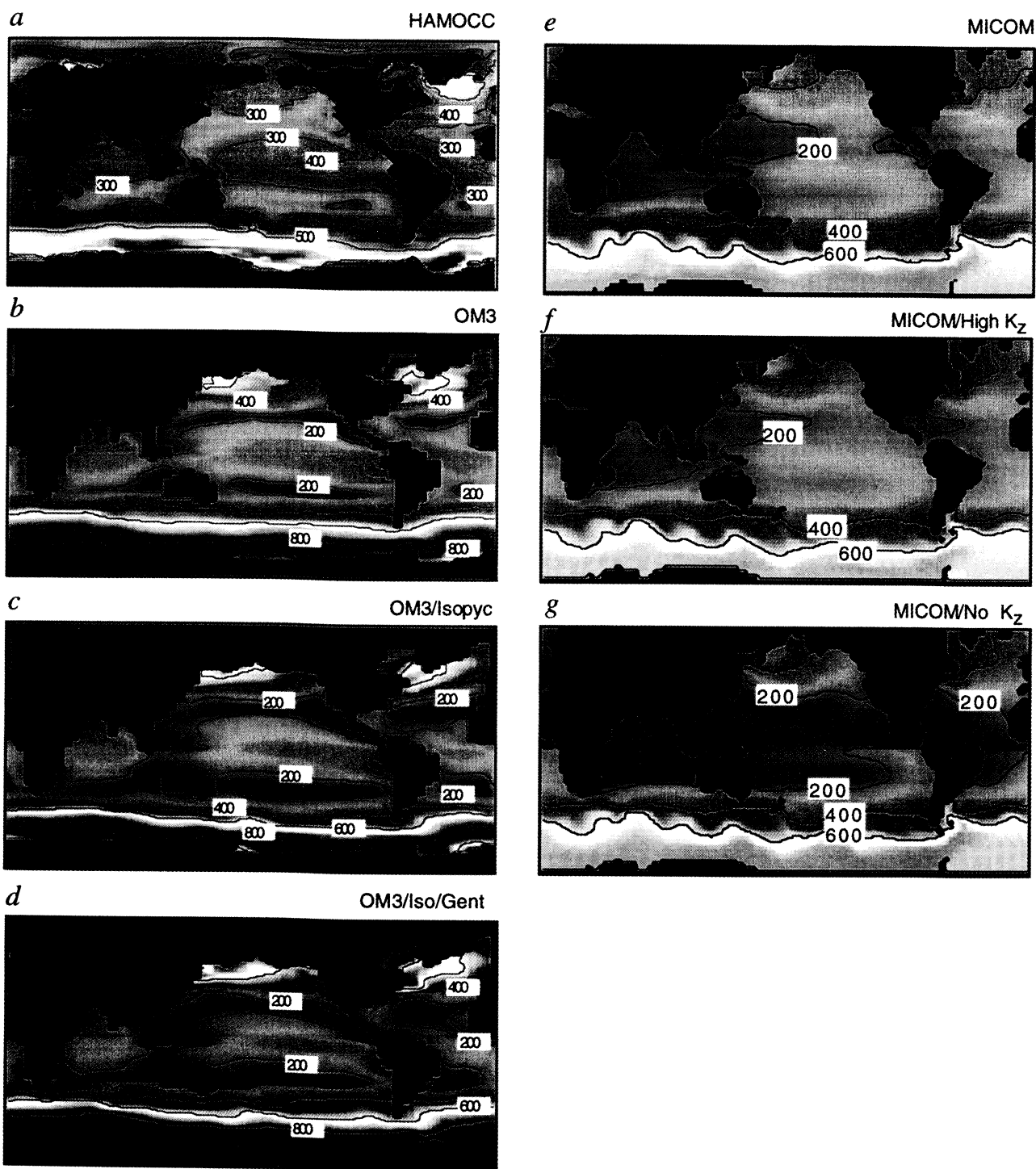


Plate 3. Results from sea-surface exposure age tracer (analogous to C) experiments from (a) HAMOCC2, (b) OM3, (c) OM3 with reoriented isopycnal diffusion following *Redi* [1982], (d) OM3 with isopycnal diffusion and *Gent and McWilliams* [1990] eddy mixing, (e) MICOM with low diapycnal mixing following *Hu* [1996], and (f) MICOM with high diapycnal K_z of 2.0 cm s.

mixing imposed by numerical schemes. Both types of models are able to reproduce the distribution of tracers such as ^{14}C in the ocean and the global ocean heat flux. It is far from trivial to say which type of model is the most reliable predictor of the behavior of the real ocean.

The question comes down to mixing between warm and cold waters in the ocean, and we have questions about both the real ocean and the numerical oceans. Field estimates of diapycnal mixing based on turbulent microstructure measurements [Gargett and Holloway, 1984] and deliberate tracer injection experiments [Ledwell et al., 1993] generally find slow rates of mixing, typically of order 0.1 cm s^{-1} , in the ocean interior. However, in the deep sea (below $\sim 1500 \text{ m}$), mixing rates are an order of magnitude faster than this can be diagnosed from the density profile of the water column [Munk, 1966]. The difference between spot measurements and large-scale diagnosis may be due to zones of higher mixing at ocean boundaries and seamounts (see Munk and Wunsch [1998]). Alternatively, Toggweiler and Samuels [1998] argue that the depths of isopycnal surfaces in the interior of the ocean are maintained by isopycnal slope across the Antarctic Circumpolar Current, rather than by vertical mixing, and that diapycnal mixing in the real ocean is very slow.

There is also observational discord near the sea surface. In contrast to deliberate tracer and microstructure estimates, various geochemical measurements imply high rates of vertical mixing, order 1 cm s^{-1} , near the sea surface. These tracers include sea surface oxygen [Spitzer and Jenkins, 1989] and helium concentrations [Jenkins, 1988] and measured rates of biological productivity limited by nutrient supply [Emerson et al., 1997; Jenkins and Wallace, 1992]. The discrepancy here might be due to frontal turbulence or transport along sloping isopycnals associated with mesoscale eddies [Mahadevan and Archer, 2000; McGillicuddy and Robinson, 1997], which might be episodic enough to be missed by the spot measurements.

An arena in which box models fall down is the prediction of new production in the ocean, which is limited by the flow of nutrients into the surface euphotic zone. Global rates of new production are shown in Figure 7 for the box models and the GCMs within which biogeochemical cycles have been implemented. These are compared with the estimate of Falkowski et al. [1998] for the real ocean. The three-box model is hobbled by the lack of resolution in the intermediate water column, forbidding shallow water column redissolution of sinking nutrients. Higher-resolution box models predict higher new production by about a factor of 2, but even these fall short of GCM and real ocean values by a further factor of 2 or more.

One concern about the GCMs is the potential for excess diapycnal mixing generated by the finite difference numerical method. Diapycnal mixing can arise from vertical numerical mixing from the vertical component of fluid flow, from horizontal mixing across sloping isopycnal surfaces, or by artificial mixing imposed to maintain numerical stability or to approximate the effects of unresolved eddies and fronts. The MICOM isopycnic ocean model is nominally superior in this regard because it eliminates by its formulation most of sources of diapycnal numerical mixing in depth-coordinate GCMs. A drawback of MICOM is that it has not yet been used for

extensive geochemical tracer studies, as have the more traditional depth-coordinate GCMs. As an interim measure, we have installed a simple sea surface C analog tracer into MICOM and several other GCMs for comparison. The tracer takes the form of an age, initialized throughout the ocean as 1000 years. At the sea surface, the age value relaxes to zero with a timescale of 0.1 yr m^{-1} , mimicking the canonical 10 year exchange time of carbon isotopes from a 100 m thick mixed layer. Throughout the ocean, the age increases at a rate of 1 yr yr^{-1} . After 100 years of simulated time, the age distribution is not in steady state, particularly in the deep sea, but the surface ocean reaches a slowly evolving balance between air-sea flux and upward mixing. This quasi-steady state is analogous to the ^{14}C age of surface water. There are some differences between the model results in Plate 3. The sea surface age of HAMOCC2 is somewhat older in the tropics and subtropics than in the other models, while OM3 is much older in the Southern Ocean than the other models. In general, however, we do not see any reason to disqualify any of the GCMs on the basis of these experiments.

Is the real ocean like a GCM or box model? GCMs are constrained by the physics of fluid flow and make detailed predictions of ocean chemistry that correspond well to the real ocean. Numerical mixing is an ongoing issue, but the consistent sea surface age and abiotic $p\text{CO}_2$ results between the isopycnic model MICOM and the depth-coordinate GCMs argues that numerical mixing is not a controlling process in determining abiotic $p\text{CO}_2$ in the level GCMs. None of the GCMs in this study resolve the eddies, fronts, internal waves and turbulence responsible for mixing in the real ocean, but the biological production estimates argue that GCMs are at least more reliable than box models (Figure 6). Nutrient [Emerson et al., 1997] and ^3He [Jenkins and Wallace, 1992] budgets in oligotrophic surface waters suggest that if anything, GCMs underestimate the long-term mean mixing near the sea surface (and hence perhaps overestimate high-

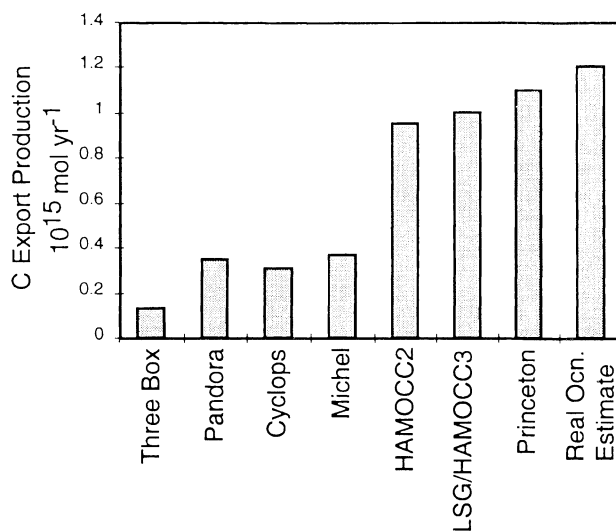


Figure 7. New production estimates from ocean models compared to the estimate of Falkowski et al. [1998] for the real ocean.

latitude $p\text{CO}_2$ sensitivity). These considerations lead us to conclude that the real ocean is probably more akin to a GCM and less to a box model.

Which GCM? The flatland model argues that abiotic CO_2 is controlled by the existence of direct pathways from the tropical surface to the deep sea, bypassing the high-latitude surface. Diapycnal mixing provides such a pathway. The desire to minimize spurious diapycnal mixing in GCMs has provoked two strategies represented in our comparison. An isopycnal coordinate system eliminates cross-grid flows except those associated with changing seawater density, which only arises from mixing in the adiabatic ocean interior. Isopycnic models are nominally the best for problems where diapycnal mixing must be explicitly controlled [Hu, 1996]. However, isopycnic models have not been extensively tested in geochemical applications.

Among depth-coordinate GCMs, Redi [1982] and Gent and McWilliams [1990] mixing eliminates diapycnal mixing by horizontal diffusion across sloping isopycnals and parameterize the effect of eddies as isopycnal diffusion. Isopycnal mixing replaces convection as a means of ventilating the deep sea (Figure 8) [Danabasoglu et al., 1994]. Circulation fields [Danabasoglu et al., 1994] and geochemistry [Gnanadesikan, 1999] in depth-coordinate GCMs generally improve with the addition of Gent and McWilliams [1990] mixing. Isopycnal mixing is supposed to allow the depth-

coordinate GCM to more closely approximate the properties of an isopycnic GCM. We have no explanation for the abiotic $p\text{CO}_2$ disagreement between OM3/Isopyc and MICOM. The MICOM result is supported by the traditional depth-coordinate GCMs, which have been the most extensively tested in geochemical studies [Heinze et al., 1999; Maier-Reimer, 1993; Najjar, 1990; Sarmiento et al., 1992]. The MICOM/traditional GCM result seems provisionally the best guess for the real ocean. However, we note that none of the models resolve eddies, which may play a role in net tracer transport [Follows and Marshall, 1996].

5. Conclusions

Atmospheric $p\text{CO}_2$ in equilibrium with an ocean GCM carbon cycle model (HAMOCC2) is less sensitive to changes in the biological pump than predicted by simpler box models of the ocean carbon cycle. $p\text{CO}_2$ sensitivity to the biological pump is determined by $p\text{CO}_2$ sensitivity to high-latitude ocean forcing because, as the biological pump efficiency increases, most of the surface chemistry change occurs in high latitudes. We use the $p\text{CO}_2$ over an abiotic ocean as a diagnostic of high-latitude sensitivity. All of the box models tested shared the high-latitude sensitivity of the three-box model, while nearly all of the GCMs lack this sensitivity, including MICOM, an isopycnal coordinate GCM that by its formulation reduces

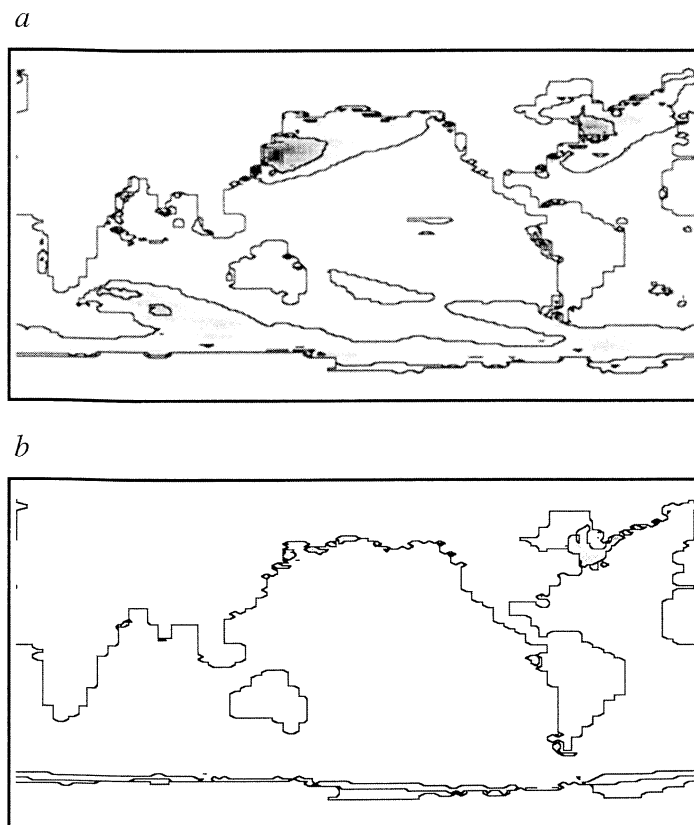


Figure 8. Rate of convective overturning in OM3 at a depth of 75 meters (a) using horizontal mixing, and (b) using Redi [1982] and Gent and McWilliams [1990] mixing. Contours at 10^5 and 10^6 watts per grid point. As noted by Danabasoglu et al., [1994], isopycnal mixing reduces the rate of convective overturning.

numerical diapycnal mixing. The only discrepancy is OM3, a depth-coordinate primitive equation model, when lateral mixing is oriented along isopycnal surfaces [Redi, 1982], which is more high-latitude sensitive than the other GCMs. This effect of isopycnal mixing needs to be tested in other depth-coordinate GCMs.

If we provisionally accept the traditional GCM/MICOM result as best guess for the behavior of the real ocean, the implication would be that pCO₂ in the real world is less dependent on high-latitude ocean forcing than was inferred from box models [Knox and McElroy, 1984; Sarmiento and Toggweiler, 1984; Siegenthaler and Wenk, 1984; Toggweiler and Sarmiento, 1985]. The implication for paleo-pCO₂ would be that a change in the efficiency of the biological pump during glacial time is insufficient to explain the pCO₂ of the glacial atmosphere [Archer et al., 2000]. The biological pump, by itself, only approaches glacial pCO₂ levels under conditions of complete sea surface nutrient depletion, conditions which do not appear to be met during the last glacial time [Boyle, 1988]. The postulated 500 Gt C release from the terrestrial biosphere during glacial time would only make matters worse, by increasing pCO₂ by ~20 μatm [Archer et al., 2000]. We would look to a change in ocean pH [Archer and Maier-Reimer, 1994; Archer et al., 2000] or nutrient inventory [Broecker and Henderson, 1998; McElroy, 1983] or some drastic rearrangement of ocean circulation [Toggweiler, 1999] to explain glacial pCO₂.

Appendix: Abiotic CO₂ Computation Details

All models were initialized with zero phosphorus to eliminate the biological pump of CO₂ from the surface to the deep ocean. Atmospheric pCO₂ and surface ocean buffer chemistry were maintained close to present-day by decreasing the mean ocean total CO₂ concentration from the observed mean of 2258 to 2085 μmol kg. Mean alkalinity was 2372 μeq kg, and initial atmospheric pCO₂ was 278 μatm. All of the models use spatially uniform (wind speed independent) piston velocities. The exchange coefficients vary somewhat from model to model, but our tests show that abiotic CO₂ is relatively insensitive to gas exchange velocities. The Pandora model has 10 boxes [Broecker and Peng, 1987], the Cyclops model has 13 [Keir, 1988], and the Michel model, derived from the flow field of a GCM, has 19 [Michel et al., 1995]. The Stocker et al. [1992] zonal mean "2.5D" model divides the ocean into Atlantic, Pacific, and Indian basins and predicts the meridional circulation of each on a grid of 7.5° with 24 points in the vertical. Advection is upwind with antidiffusion corrections [Smolarkiewicz and Grabowski, 1990]. K_z is 3 cm² s⁻¹. The Princeton model is an abiotic simulation from Murnane et al. [1999] using on-line center-difference tracer advection and a grid resolution of ~4°. K_z ranges from 0.3 – 1.0 cm² s⁻¹. The advantage of advecting tracers immediately with calculation of the flow field ("on-line") is a better representation of the effects of episodic convection on tracer transport. OM3 (as yet undocumented in the literature) is a depth-coordinate free-surface model following Killworth et al. [1991], and was obtained from John Anderson at the University of Wisconsin, by personal communication (1998). The model uses message passing for parallel architectures. The

model uses center differencing on a 1.5° × 3° × 15 level unstaggered A-grid. K_z is based on Pacanowski and Philander [1981] with a background of 0.1 cm² s⁻¹. Tracer advection is on-line. Experiment OM3 uses Cartesian horizontal mixing. Lateral diffusion is oriented to local isopycnal surfaces in experiment OM3/Isopyc [Redi, 1982], and isopycnal thickness diffusion [Gent and McWilliams, 1990] is added to this in experiment OM3/Iso-GM. HAMOCC2 is an off-line tracer advection code with a 1 year time step [Maier-Reimer and Bacastow, 1990], using an implicit upstream method. Vertical mixing is numerical, probably of similar magnitude to LSG (1.6 cm² s⁻¹). LSG is an on-line calculation which resolves the seasonal cycle [Winguth et al., 1994]. Vertical mixing is numerical and has been measured to be 1.6 cm² s⁻¹ [Maier-Reimer et al., 1993]. The Gent and McWilliams [1990] eddy mixing scheme (added to LSG/HAMOCC3/GM by Uwe Mikolajewicz, personal communication, 1998), does not include Redi [1982] isopycnal diffusion reorientation. MICOM [Bleck and Smith, 1990] is an isopycnal ocean circulation model, here run at 2.8° resolution with seasonal forcing. We used a parallelized version of the code called SC-MICOM [Bleck et al., 1995]. MICOM is the only GCM in the comparison which resolves a surface ocean mixed layer of arbitrary thickness, using a Kraus Turner [1967] TKE model. Tracer advection is on-line using upstream differences with antidiffusion corrections [Smolarkiewicz and Grabowski, 1990]. Numerical diapycnal diffusion is eliminated by the isopycnal coordinate system, and explicit diapycnal diffusion ranges from 0.1 to 1.0 cm² s⁻¹ [Hu, 1996]. The passive tracer (e.g., CO₂) advection code was upgraded to the same leapfrog scheme that is used for salinity in MICOM, decreasing execution speed somewhat but drastically improving tracer conservation. Diapycnal diffusion of tracers is handled independently from salinity and density, enabling us to test the effect of no tracer diffusion ("no K_z ") and uniform K_z of 1 cm² s⁻¹ ("high K_z ").

Acknowledgements. We thank Jorge Sarmiento, Robbie Toggweiler, and two anonymous reviewers for thoughtful and productive discussion.

References

- Archer, D. E., and E. Maier-Reimer, Effect of deep-sea sedimentary calcite preservation on atmospheric CO₂ concentration, *Nature*, 367, 260-264, 1994.
- Archer, D. E., A. Winguth, D. Lea, and N. Mahowald, What caused the glacial / interglacial atmospheric pCO₂ cycles?, *Rev. Geophys.*, 38, 159-189, 2000.
- Bacastow, R. B., The effect of temperature change of the warm surface waters of the oceans on atmospheric CO₂, *Global Biogeochem. Cycles*, 10, 319-334, 1996.
- Barnola, J. M., D. Raynaud, Y. S. Korotkevich, and C. Lorius, Vostok ice core provides 160,000 year record of atmospheric CO₂, *Nature*, 329, 408-414, 1987.
- Bleck, R., and L. T. Smith, A wind-driven isopycnal coordinate model of the North and Equatorial Atlantic Ocean, 1. Model development and supporting experiments, *J. Geophys. Res.*, 95, 3273-3285, 1990.
- Bleck, R., S. Dean, M. O'Keefe, and A. Sawdey, A comparison of data-parallel and message-passing versions of the Miami Isopycnal Coordinate Ocean Model (MICOM), *Parallel Comput.*, 21, 1695-1720, 1995.
- Boyle, E. A., Vertical oceanic nutrient fractionation and glacial/interglacial CO₂ cycles, *Nature*, 331, 55-56, 1988.
- Broecker, W. S., and G. Henderson, The sequence of event surrounding

- termination II and their implications for the cause of glacial-interglacial CO₂ changes, *Paleoceanography*, *13*, 352-364, 1998.
- Broecker, W. S., and T. H. Peng, The role of CaCO₃ compensation in the glacial to interglacial atmospheric CO₂ change, *Global Biogeochem. Cycles*, *1*, 15-29, 1987.
- Broecker, W., J. Lynch-Stieglitz, D. Archer, M. Hofmann, E. Maier-Reimer, O. Marchal, T. Stocker, and N. Gruber, How strong is the Harvardton-Bear constraint?, *Global Biogeochem. Cycles*, *13*, 817-821, 1999.
- Danabasoglu, G., J. C. McWilliams, and P. R. Gent, The role of mesoscale tracer transports in the global ocean circulation, *Science*, *264*, 1123-1126, 1994.
- Emerson, S., P. Quay, D. Karl, C. Winn, L. Tupas, and M. Landry, Experimental determination of the organic carbon flux from open-ocean surface waters, *Nature*, *389*, 951-954, 1997.
- Falkowski, P. G., R. T. Barber, and V. Smetacek, Biogeochemical controls and feedbacks on ocean primary production, *Science*, *281*, 200-206, 1998.
- Follows, M. J., and J. C. Marshall, On models of bomb ¹⁴C in the North Atlantic, *J. Geophys. Res.*, *101*, 22,577-22,582, 1996.
- Gargett, A. E., and G. Holloway, Dissipation and diffusion by internal wave breaking, *J. Mar. Res.*, *42*, 15-27, 1984.
- Gent, P., and J. C. McWilliams, Isopycnal mixing in ocean circulation models, *J. Phys. Oceanogr.*, *20*, 463-474, 1990.
- Gnanadesikan, A., A global model of silica cycling: Sensitivity to eddy parameterization and remineralization, *Global Biogeochem. Cycles*, *13*, 199-220, 1999.
- Heinze, C., E. Maier-Reimer, A. M. E. Winguth, and D. Archer, A global oceanic sediment model for long term climate studies, *Global Biogeochem. Cycles*, *13*, 221-250, 1999.
- Hu, D., On the sensitivity of thermocline depth and meridional heat transport to vertical diffusivity in OGCMs, *J. Phys. Oceanogr.*, *26*, 1480-1494, 1996.
- Jenkins, W. J., Nitrate flux into the euphotic zone near Bermuda, *Nature*, *331*, 521-524, 1988.
- Jenkins, W. J., and D. W. R. Wallace, Tracer based inferences of new primary production in the sea, in *Primary Productivity and Biogeochemical Cycles in the Sea*, edited by P. G. Falkowski and A. D. Woodhead, pp. 299-316, Plenum, New York, 1992.
- Keir, R. S., On the late Pleistocene ocean geochemistry and circulation, *Paleoceanography*, *3*, 413-445, 1988.
- Killworth, P. D., D. Stannforth, D. J. Webb, and S. M. Paterson, The development of a free-surface Bryan-Cox-Semtner ocean model, *J. Physical Oceanogr.*, *21*, 1333-1348, 1991.
- Knox, F., and M. McElroy, Change in atmospheric CO₂: Influence of the marine biota at high latitude, *J. Geophys. Res.*, *89*, 4629-4637, 1984.
- Kraus, E. B., and J. S. Turner, A one-dimensional model of the seasonal thermocline, II, The general theory and its consequences, *Tellus*, *19*, 98-105, 1967.
- Ledwell, J. R., A. J. Watson, and C. S. Law, Evidence for slow mixing across the pycnocline from an open-ocean tracer release experiment, *Nature*, *364*, 701-703, 1993.
- Levitus, S., M. E. Conkright, J. L. Reid, R. G. Najjar, and A. Mantyla, Distribution of nitrate, phosphate, and silicate in the world's oceans, *Prog. Oceanogr.*, *31*, 245-273, 1993.
- Mahadevan, A., and D. Archer, Effect of mesoscale circulation on nutrient supply to the upper ocean, *J. Geophys. Res.*, *105*, 1209-1225, 2000.
- Maier-Reimer, E., Geochemical cycles in an ocean general circulation model. Preindustrial tracer distributions, *Global Biogeochem. Cycles*, *7*, 645-678, 1993.
- Maier-Reimer, E., and R. Bacastow, Modelling of geochemical tracers in the ocean, in *Climate-Ocean Interaction*, edited by M. E. Schlesinger, pp. 233-267, Kluwer Acad., Norwell, Mass, 1990.
- Maier-Reimer, E., U. Mikolajewicz, and K. Hasselmann, Mean circulation of the Hamburg LSG OGCM and its sensitivity to the thermohaline surface forcing, *J. Phys. Oceanogr.*, *23*, 731-757, 1993.
- Martin, J. H., and S. E. Fitzwater, Iron deficiency limits phytoplankton growth in the north-east Pacific subarctic, *Nature*, *331*, 341-343, 1988.
- McElroy, M. B., Marine biological controls on atmospheric CO₂ and climate, *Nature*, *302*, 328-329, 1983.
- McGillcuddy, D. J., and A. R. Robinson, Eddy induced nutrient supply and new production in the Sargasso Sea, *Deep Sea Res. Part I*, *44*, 1427-1450, 1997.
- Michel, E., L. D. Labeyrie, J.-C. Duplessy, N. Gorfu, M. Labracherie, and J.-L. Turon, Could deep subantarctic convection feed the world deep basins during the last glacial maximum, *Paleoceanography*, *10*, 927-942, 1995.
- Munk, W. H., Abyssal recipes, *Deep Sea Res.*, *13*, 207-230, 1966.
- Munk, W., and C. Wunsch, Abyssal recipes II. energetics of tidal and wind mixing, *Deep Sea Res Part I*, *45*, 1977-2010, 1998.
- Murnane, R. J., J. L. Sarmiento, and C. LeQuere, The spatial distribution of air-sea CO₂ fluxes and the interhemispheric transport of carbon by the oceans, *Global Biogeochem. Cycles*, *13*, 287-305, 1999.
- Najjar, R. G., Simulations of the phosphorous and oxygen cycles in the world ocean using a general circulation model, Princeton Univ., Princeton N.J., 1990.
- Pacanowski, R. C., and S. G. H. Philander, Parameterization of vertical mixing in numerical models of tropical oceans, *J. Phys. Oceanogr.*, *11*, 1443-1451, 1981.
- Peng, T. H., and W. S. Broecker, Factors limiting the reduction of atmospheric CO₂ by iron fertilization, *Limnol. Oceanogr.*, *36*, 1919-1927, 1991.
- Redi, M. H., Oceanic isopycnal mixing by coordinate rotation, *J. Phys. Oceanogr.*, *12*, 1154-1158, 1982.
- Sarmiento, J. L., and J. C. Orr, Three-dimensional simulations of the impact of Southern Ocean nutrient depletion on atmospheric CO₂ and ocean chemistry, *Limnol. Oceanogr.*, *36*, 1928-1950, 1991.
- Sarmiento, J. L., U. Siegenthaler, and J. C. Orr, A perturbation simulation of CO₂ uptake in an ocean general circulation model, *J. Geophys. Res.*, *97*, 3621-3645, 1992.
- Sarmiento, J. L., and R. Toggweiler, A new model for the role of the oceans in determining atmospheric pCO₂, *Nature*, *308*, 621-624, 1984.
- Siegenthaler, U., and T. Wenk, Rapid atmospheric CO₂ variations and ocean circulation, *Nature*, *308*, 624-626, 1984.
- Smolarkiewicz, P. K., and W. W. Grabowski, The multidimensional positive definite advection transport algorithm: Further development and applications, *J. Comput. Phys.*, *67*, 396-438, 1990.
- Spitzer, W. S., and W. J. Jenkins, Rates of vertical mixing, gas exchange, and new production: Estimates from seasonal gas cycles in the upper ocean near Bermuda, *J. Mar. Res.*, *47*, 169-196, 1989.
- Stocker, T. F., D. G. Wright, and L. A. Mysak, A zonally averaged, coupled ocean-atmosphere model for paleoclimatic studies, *J. Clim.*, *5*, 773-797, 1992.
- Toggweiler, J. R., Variation of atmospheric CO₂ by ventilation of the ocean's deepest water, *Paleoceanography*, *14*, 571, 1999.
- Toggweiler, J. R., and B. Samuels, On the ocean's large-scale circulation near the limit of no vertical mixing, *J. Phys. Oceanogr.*, *28*, 1832-1852, 1998.
- Toggweiler, J. R., and J. L. Sarmiento, Glacial to interglacial changes in atmospheric carbon dioxide: the critical role of ocean surface water in high latitudes, in *The Carbon Cycle and Atmospheric CO₂: Natural Variations Archaean to Present*, vol. 32, edited by E. T. Sundquist and W. S. Broecker, pp. 163-184, AGU, Washington, D.C., 1985.
- Winguth, A. M. E., M. Heimann, K. D. Kurz, E. Maier-Reimer, U. Michajewicz, and J. Segsneider, ENSO related fluctuations of the marine carbon cycle, *Global Biogeochem. Cycles*, *8*, 39-65, 1994.

D. Archer, G. Eshel, R. Jacob, and R. Pierrehumbert, Department of the Geophysical Sciences, University of Chicago, Chicago, IL 60637. (d-archer@uchicago.edu)

W. Broecker, Lamont Doherty Earth Observatory, Columbia University, Palisades, NY 10964.

M. Tobis, Space Science and Engineering Center, University of Wisconsin, Madison, WI 53706.

A. Winguth, Department of Atmospheric and Oceanic Sciences, University of Wisconsin, Madison, WI 53706.

(Received August 20, 1999; revised March 1, 2000; accepted March 7, 2000.)